Calibration, Repeatability, and Interpretation of In-Situ Tectonic Stress Measurements from Wireline Straddle Packer MicroFrac Testing: Case Study of an Onshore Field in the UAE*

Dee A. Moronkeji[1], Javier A. Franquet[3], Steve Smith[3], Umesh Prasad[2], Noora S. Al-Shehhi[4], and Mohamed El-Hamawi[4]

Search and Discovery Article #41635 (2015)
Posted June 29, 2015

*Adapted from extended abstract prepared in conjunction with poster presentation at AAPG Annual Convention & Exhibition 2015, Denver, Colorado, May 31-June 3, 2015.

[1]Baker Hughes, Houston, TX, United States (dee.moronkeji@bakerhughes.com)
[2]Baker Hughes, Houston, TX, United States
[3]Baker Hughes, Abu Dhabi, United Arab Emirates
[4]Abu Dhabi Company for Onshore Oil Operations, Abu Dhabi, United Arab Emirates

Abstract

Wireline straddle packer microfrac tests for in-situ stress characterization have become an important technology to identify the best place to fracture during the drilling and completion of oil and gas wellbores. The microfrac testing procedure includes formation breakdown, fracture propagation, fracture reopening cycles, and pressure fall-off cycles for fracture closure identification.

The objective of this microfrac testing was to validate and calibrate the horizontal stress profile in various intervals of the target formation. This paper will focus on the calibration and repeatability of microfrac tests to obtain quantitative downhole formation breakdown, fracture re-opening, fracture propagation, and fracture closure pressure in a vertical borehole located onshore Abu Dhabi. A pre-job assessment was conducted to identify preferable intervals, which took into consideration the borehole conditions, the straddle packer capabilities, and limitations so as to design a successful micro-fracturing job.

Three fracture propagation and pressure fall-off cycles were analyzed to measure the fracture closure pressure. The results were used to calibrate the far-field minimum horizontal stress profile. Fracture closure was obtained by natural leak-off pressure decline behavior; no flow-back was required to induce fracture closure. The fracture closure pressure was identified by three different methods: (I) Square root of time (SRT) pressure decline analysis using the isolated interval pressure vs square-root of shut-in time, (II) Log-Log pressure decline analysis using the pressure derivative of the delta pressure and delta time in log-log plot, and (III) G-function analysis by plotting the GdP/dG on a pressure vs G-time plot.

The results show how crucial it is that the inflatable elements are positioned on layers with stress contrast in respect to the isolated formation interval so that optimum fracture containment and proper fracture propagation are obtained. This is important in order to avoid sleeve

fracturing and early hydraulic communication between the fracture and the hydrostatic pressure. The repeatability and interpretation of the microfrac testing for validation and calibration of horizontal stresses and stress contrast are discussed as well as the importance of the static elastic properties of the rock to improve the lateral strain values in reproducing the fracturing pressure recorded on the microfrac tests.

Introduction

The study well is in an onshore field south of Abu Dhabi, in the rolling sand dunes north of the Liwa oasis. The field is a significant contributor of oil and gas production in the region. The objective of the microfracture tests (in this study) is to measure the in-situ stress acting in the gas producing zone of the well. The tests comprise measuring the fracture initiation, propagation, reopening, and closure pressures in the target formation to validate and calibrate the horizontal stress profile.

Formation breakdown, fracture propagation, fall off, and three repeat cycles of fracture reopening, fracture propagation, and pressure fall-off were performed for each station during the microfrac testing procedure. No flow-back was required to induce fracture closure in the study because the formation is permeable enough for natural leak-off. Borehole quality is an important factor to consider during the positioning of the wireline straddle packer. The sealing capacity of the inflatable elements against the formation can be compromised by borehole washouts and extensive breakouts (Franquet et al., 2010). Rubber deterioration during inflation, deforming the elements, is a possibility and must be minimized by avoiding intervals of extreme borehole wall rugosity. Figure 1 shows the recommended workflow for successful wireline straddle packer micro-fracture testing:

1. Pre-job assessment and interval selection.
2. Real-time monitoring.
3. Post-acquisition pressure decline analysis.
4. Validation of in-situ horizontal stresses by adjusting lateral tectonic strains.

Pre-Job Micro-fracture Assessment and Interval Selection

The pre-job micro-fracture assessment was performed in a nearby offset well. The objective of the assessment is to estimate the rock strength, pore pressure, in-situ stress magnitude and fracturing pressure to compare the predicted formation breakdown pressure against the differential pressure capability of the straddle packer tool.

Griffith, 1921, describes the mechanics of fracture propagation analytically in Equations (1) and (2):

$$\frac{\delta U}{\delta a} = 2G \quad (1)$$

$$G = \frac{\pi\sigma^2 a}{E} \quad (2)$$

where U is the energy used to produce elastic stress, a is the characteristic fracture length, G is the crack driving force, σ is the far-field stress and E is the Young's Modulus of the rock where cracks propagate.

The Griffith equations show that estimating the rock elastic properties and in-situ stress magnitude is important because rock with high Young's modulus requires less energy for fracture propagation while intervals with high horizontal stresses require more energy to propagate a hydraulic fracture. The rock elastic properties and in-situ stress magnitude can be obtained during a pre-job micro-fracture assessment and used to identify the correct intervals to micro-fracture with the straddle packer tool. Horizontal stress magnitude profiles can be estimated from rock stiffness tensor, Biot's poroelastic parameter, pore pressure, overburden stress, and lateral tectonic strains in isotropic or anisotropic rocks (Franquet and Rodriguez 2012). The log-derived stress profile can be used to select the best intervals for microfrac testing that show adequate stress contrast for inducing a contained small fracture between the elements and avoiding sleeve fracturing. The methodology helps reduce the risk of inducing a fracture at the packer position and increase the chances for a successful micro-fracture job by reducing the nonproductive logging time. The micro-fracture test selection involves the identification of a 1-m interval with natural fracture propagation barriers above and below the straddle packers' position.

The borehole diameter for the study well is 6 in and the wireline micro-fracture tests are performed in an open hole condition. The overburden gradient (OBG) is estimated as 1.05 psi/ft by integrating the density log up to the surface on a nearby well. The rock is assumed to be isotropic and linear-elastic using the isotropic rock model (ISO). The formation breakdown was estimated assuming no fluid invasion into the formation with a perfect impermeable borehole wall condition. A mud weight of 11 ppg with high chloride content is employed, and the pore pressure profile is estimated as 0.469 psi/ft. The horizontal stresses are estimated using the lateral tectonic strain model (lateral strains in the direction of $\sigma_{h,min}$ and $\sigma_{H,max}$ as 0.1 and 0.4 mStrain, respectively). The lateral strain values are obtained from previous micro-fracture tests performed in Abu Dhabi, where the lateral tectonic strains were calibrated (Ihab et al., 2014).

The rock stiffness was converted from dynamic (acoustically derived) to static (triaxial compression) using the Lacy's empirical correlation (Lacy 1997) for Young's modulus (while a 5% reduction was applied for Poisson's ratio). The target Stations 1 and 2 comprised low density and high porosity, with an estimated unconfined compressive strength (UCS) of 10,500 psi, a Young's modulus (EMODX) of 3 Mpsi, and Poisson's ratio (POISYX) of 0.25. Figure 2 shows the pre-job micro-fracture assessment performed from logging data of an offset well.

The first track in Figure 2 shows the gamma ray curve and caliper log used to identify potential zones where washouts or bad borehole conditions can be expected. The next tracks (from left to right) the vertical fracture migration and shows the net pressure necessary to propagate a hydraulic-induced fracture from low stress intervals (and is illustrated with pink zones). As the net pressure increases, the intervals are color-coded from green to blue to grey to red. The grey and red zones correspond to the high stress zones, while green and blue are the transition zones between low and high horizontal stress.

The third track of Figure 2 shows the static-derived components of the stiffness tensor "C_{ij}", indicating the compressional components in black, the shear components in red, and the non-diagonal components in green, (Franquet et al., 2011). The track indicates the type of anisotropic rock model used in horizontal stress estimation and the zones with high stiffness. The stress and pore pressure profiles in gradient values are plotted next to the rock-estimated mechanical properties. The sixth track corresponds to the stress contrast, where high-stress intervals are highlighted in blue while the low stress intervals are indicated in red. Finally, the last track shows the overburden stress, horizontal stresses, pore pressure, hydrostatic pressure, and predicted formation breakdown pressure in yellow and the maximum pressure between the packers in black. Zones highlighted in green indicate that the straddle packer has enough differential pressure to break the testing intervals. The pre-job micro-fracture assessment illustrates few tight zones that require higher differential pressure than the straddle packer tool capability (based on the hydrostatic pressure used in the well and the assumed lateral tectonic strains). If the tight zones must be micro-fracture tested, the hydrostatic pressure has to be increased by 1000 psi from the well head at the time of testing.

Microfrac Test Results

The micro-fracture test is performed at two depth intervals (Stations 1 and 2) in the target zones. The absolute bottom hole pressure (APQJ) of the isolated interval and the absolute pressure (ASPEP) inside the packers are denoted in blue and magenta, respectively (Figure 3 for Station 1). The flow rate is a red line (cc/s) and the cumulative displaced volume is plotted in green (liters). The bottom hole temperature is a dark brown line (°F).

At Station 1 (top interval), the straddle packers are inflated in about 18 minutes using a 500-cc stroke volume pump, with an average flow rate of 10 cc/s. The borehole temperature was approximately 262 °F and the hydrostatic pressure was 5100 psi.

Two packer sealing tests were performed at the station by injecting up to 5700 psi of differential pressure across the packers (600 psi above hydrostatic pressure). The formation breakdown is observed at 8200 psi, with 3100 psi of differential pressure applied across the packers; the pressure drop in the APQJ during injection in the isolated interval indicates formation breakdown. The fracture is propagated for approximately 6 minutes after formation breakdown in the first pressurization cycles (FOT1); pressure declines rapidly after shut-in, indicating high leak-off. After the pressure decline in FOT1, the fracture was reopened in three more pressurization cycles (FOT2, FOT3 and FOT4) to propagate the fracture far enough away from the well and beyond the influence of the near borehole induced stresses.

FOT2 shows the reopening pressure at 8400 psi, 200 psi above the breakdown pressure in FOT1, and the fracture propagated for approximately 9 minutes and was shut-in. The pressure declined naturally for about 14 minutes to reach a good fracture closure measurement. The reopening pressure at FOT3 was 8200 psi, similar to the breakdown pressure at FOT1, and propagated for 24 minutes. FOT4 shows the reopening pressure at 8000 psi; because it is the last pressurization cycle, the shut-in period declined naturally for more than 35 minutes to obtain a good fracture closure. The last cycle also shows stable fracture propagation without a significant increment in fracture propagation pressure. The last cycle is used to calculate fracture closure pressure because it is considered the most reliable measurement of the far-field minimum horizontal stress (the fracture is propagated further away from the influence of the borehole-induced stresses).

At Station 2 (bottom interval), the straddle packers are inflated in about 10 minutes using a 500 cc stroke volume pump, with an average flow rate of 10 cc/s. The borehole temperature was approximately 262 °F and the hydrostatic pressure was 5175 psi. The micro-fracture test comprised one packer sealing test and four pressurization cycles (as performed previously in Station 1). The packer integrity test was performed at 600 psi above the hydrostatic pressure.
Figure 4 shows the formation breakdown in the first pressurization cycle (FOT1) at 8100 psi. Station 2 shows a text-book example of formation breakdown on a brittle rock, compared with the breakdown pressure observed in Station 1, which is less obvious.

The drop between the breakdown pressure and the subsequent fracture reopening pressures was approximately 500 psi, indicating an estimated rock tensile strength of 500 psi. The three re-opening pressures in the second, third, and fourth pressurization cycles (FOT2, FOT3, and FOT4) are observed at 7700, 7800, and 7800 psi, respectively, showing a consistent recurrence of fracture reopening. The fracture closure is analyzed in all four pressurization cycles. There is a typical decrease in fracture closure pressure as the fracture is propagated further away from the borehole during the subsequent pressurization cycles.

The pressure decline behavior from FOT1 and FOT4 shows the isolated interval pressure reaching values lower than the hydrostatic pressure at the end of the decline (indicating the interval pressure is approaching the reservoir pressure and the straddle packer elements are sealing properly at the borehole wall). The last pressurization cycle shows stable fracture propagation with some propagation resistance.

Pressure Decline Analysis of MicroFrac Testing

Four fracture propagation and pressure fall-off cycles are analyzed on each station to measure fracture closure pressures. The fracture closure was obtained by natural leak-off pressure decline behavior and no flow-back was required to induce fracture closure. There are several fracture closure pressure analysis methods available to estimate fracture closure pressure (Fairhurst 1964; De Bree and Walters 1989; Thiercelin et al., 1993; Guo et al., 1993; and Barree et al., 2007). The fracture closure pressure is identified using three methods:

1. Square-root of time (SRT) pressure decline analysis uses the isolated interval pressure versus the square-root of shut-in time,
2. Log-log pressure decline analysis uses the pressure derivative of the delta pressure and delta time in log-log plot, and
3. G-function analysis plots the GdP/dG on a pressure versus G-time plot.

Each fall-off cycle is identified with the three decline analysis methods to reach the more robust fracture identification. The first method considers a linear regression behavior at the early stage of the shut-in time and the fracture closure pressure is associated with the deviation from the linear pressure decline behavior. To identify the peak of the curve, as a guide for fracture closure picking, plot the square-root of shut-in time multiplied by the pressure derivative in the square-root of time (t-1/2dP/dt-1/2).

The second method looks for a change in the slope of the pressure derivative d (log dP)/d (log dt) from a linear behavior around 0.5 slope into a decreasing trend (the change is associated with fracture closure). The pressure derivative curve must be around 0.5 for a dominant infinite-conductivity fracture flow regime (Jones and Sargeant 1993) when the fracture is still open; the pressure derivative decreases as the fracture

closes.

The final method looks for a change in the behavior in the pressure versus G-function plot by identifying the change of slope of the GdP/dG derivative curve from linear increasing to flat or a decreasing trend. Figure 5 and Figure 6 show the fracture closure identification for each method on the last
injection cycle for both micro-fracture stations.

The fracture closure pressure summary table is presented for all cycles in Stations 1 and 2 in Table 1. Table 1 illustrates the good repeatability in the fracture reopening pressure and propagation pressure from the micro-fracture straddle packer tool.

The repeatability is a result of the pre-job assessment which helped identify preferable intervals in the formation of interest. Also important are borehole conditions and the placement of the straddle packer to avoid deterioration of the rubber during inflation and deflation of the elements. Positioning the straddle packer on layers with stress contrast with respect to the isolated formation interval to avoid sleeve fracturing and early hydraulic communication between the fracture and the hydrostatic pressure is also crucial to obtaining good repeatability in fracture reopening and propagation.

Tectonic Strain Calibration and Repeatability from Post-Job Analysis

Repeatability of micro-fracture tests to obtain quantitative and reliable downhole formation breakdown, fracture re-opening, fracture propagation, and fracture closure pressures in a vertical borehole is important for calibrating the magnitude of in-situ horizontal stresses. The interpretation of micro-fracture fall-off tests for fracture closure pressure identification and quantification of the horizontal stress contrast between a reservoir and tight zones are useful in building a realistic geomechanical model. The methodology for acquiring the tectonic stress in the model is obtained by adding two lateral tectonic strains in the minimum and maximum horizontal stress directions.

The lateral tectonic strain is achieved by specifying the tectonic strain values in the direction of $\sigma_{h,min}$ and $\sigma_{H,max}$ to reproduce the formation breakdown and fracture closure at each micro-fracture depth.

The stress profile does not include the thermal effect because it is assumed to be negligible (in this study). The post-job tectonic strain calibration is performed using the constitutive isotropic (ISO) rock model for stress calibration and the micro-fracture results from the two stations. It is important to convert dynamic elastic properties to static stiffness properties before performing the tectonic lateral strain calibration to avoid underestimating the values of the tectonic strains to reproduce the magnitude of in-situ stresses measured by the straddle packer tool (Ihab et al., 2014).

The ISO model stiffness tensor can be derived from DTC and DTS, as shown in Equations (3), (4), and (5):

$$C_{11} = C_{22} = C_{33} = \rho\left(\frac{1}{DTC}\right)^2 \times CF$$

(3)

$$C_{12} = C_{13} = C_{23} = C_{11} - 2C_{44}$$

(4)

$$C_{44} = C_{55} = C_{66} = \rho\left(\frac{1}{DTS}\right)^2 \times CF$$

(5)

where C_{11} is the compressional stiffness tensor component (Mpsi), C_{12} is the non-diagonal stiffness tensor component (Mpsi), DTC is the compressional wave slowness (μs/ft), DTS is the shear wave slowness (μs/ft), and CF is the unit conversion factor = 13474.44 to obtain (Mpsi) when density is in (g/cc) and the slowness is in (μs/ft). The ISO model estimates the horizontal stresses using constant lateral tectonic strain values of -0.05 and 0.3 mStrain in the direction of $\sigma_{h,min}$ and $\sigma_{H,max}$, respectively. The horizontal stress profiles are calculated with the following equations for isotropic formations (Franquet and Rodriguez 2012) using the static log-derived stiffness tensor components:

$$\sigma_{h,min} = \frac{C_{12}}{C_{11}}(\sigma_v - \alpha P_P) + \alpha P_p + \left(C_{11} - \frac{C_{12}^2}{C_{11}}\right)\varepsilon_h + \left(C_{12} - \frac{C_{12}^2}{C_{11}}\right)\varepsilon_H$$

(6)

$$\sigma_{H,max} = \frac{C_{12}}{C_{11}}(\sigma_v - \alpha P_P) + \alpha P_p + \left(C_{11} - \frac{C_{12}^2}{C_{11}}\right)\varepsilon_H + \left(C_{12} - \frac{C_{12}^2}{C_{11}}\right)\varepsilon_h$$

(7)

where ε_h is the minimum lateral tectonic strain (mStrain), ε_H is the maximum lateral tectonic strain (mStrain), σ is the far-field stress (psi), $\sigma_{h,min}$ is the minimum horizontal stress magnitude (psi) and $\sigma_{H,max}$ is the maximum horizontal stress magnitude (psi).

Figure 7 shows the post-job calibration using the ISO model. The plot shows the good agreement between the fracture closure measurements from the straddle packer micro-fracture tests and the estimated minimum horizontal stress. There is good agreement between the predicted formation breakdown pressure from the horizontal stress model and the straddle packer measurements. The two in-situ measurements (formation breakdown and fracture closure) constrain the magnitude of the horizontal stresses in the formation. Good agreement between the model and measurements must be obtained for both stations to obtain continuous minimum and maximum horizontal stress profiles in the well.

Track positions are the same as in Figure 2, except that track 7 includes the calibration points from reservoir build-up testing (blue dots) [PPG curve is not localized fluid gradient], fracture closure (red triangles) and formation breakdown (orange diamonds), from the straddle packer micro-fracture testing.

Conclusions

The importance of the pre-job assessment to estimate rock strength, in-situ horizontal stress magnitude, and formation breakdown pressure is to verify the wireline straddle packer tool has sufficient differential pressure to initiate a fracture between the elements. The pre-job assessment also helps to identify intervals that have a proper stress contrast between the testing interval and the surrounding formations to minimize the risk of sleeve fracturing at the packer positions.

The fracture closure estimation from the pressure decline analysis shows that the square-root of shut-in time pressure decline analysis always provides a lower fracture closure estimate than the Log-log pressure derivative and G-function decline analysis. The first station did not reach a repeated final fracture closure, indicating that a fifth pressurization cycle was necessary to validate the last fracture closure point; the fracture closure at the last cycle (FOT4) was similar to the closure observed in the previous fall-off test (FOT3) in Station 2.

The use of lateral tectonic strain in the isotropic model helped when calibrating the minimum and maximum horizontal stress magnitude (using -0.05 and 0.3 mStrain for the tectonic lateral strains). The negative tectonic strain suggests the reservoir is relaxed in the direction of minimum horizontal stress within an extensional tectonic state. The positive lateral strain indicates the reservoir is within a compressional tectonic state in the direction of the maximum horizontal stress. The in-situ stress state obtained from the micro-fracture measurements suggests that the reservoir is within a normal faulted stress regime, where both horizontal stresses are lower than the overburden stress.

Acknowledgements

The authors thank ADCO and Baker Hughes for permission to publish these results.

References Cited

Barree, R.D., V.L. Barree, and D.P. Craig, 2007, Holistic Fracture Diagnostics: SPE Paper 107877, Rocky Mountain Oil and Gas Technology Symposium, Denver, Colorado, 16-18 April.

Castillo, J.L., 1987, Modified Fracture Pressure Decline Analysis Including Pressure-Dependent Leakoff: SPE Paper 16417, SPE/DOE Low Permeability Reservoirs Symposium, Denver, Colorado, 18-19 May.

De Bree, P., and J.V. Walters, 1989, Micro/Minifrac Test Procedures and Interpretation for In Situ Stress Determination: Int. J. Rock Mech. Min. Sci. & Geomech., v. 26, p. 515-521.

Fairhurst, C., 1964, Measurement of In Situ Rock Stresses, with Particular Reference to Hydraulic Fracturing: Rock Mech. Eng. Geology, v. 2, p. 129-149.

Franquet, J.A., I. Gaz, F. Ibragimov, A. Seryakov, and J. Huthwaite, 2010, Caprock Integrity Testing Through Openhole Micro-Fracturing in

Caspian Sea Sub-Salt Formations: 10th Offshore Mediterranean Conference and Exhibition, Ravenna, Italy, 23-25 March.

Franquet, J.A., D. Patterson, and D. Moos, 2011, Advanced Dipole Borehole Acoustic Processing – Rock Physics and Geomechanics Applications: SEG paper 2011-1876, 81st Society of Exploration Geophysicists Annual Meeting and International Exposition, San Antonio, Texas, 18-23 September.

Franquet, J.A., and E.F. Rodriguez, 2012, Orthotropic Horizontal Stress Characterization from Logging and Core-Derived Acoustic Anisotropies: Paper ARMA 12-644, 46th U.S. Rock Mechanics/Geomechanics Symposium, Chicago, Illinois, 24-27 June.

Griffith, A.A., 1921, The Phenomena of Rupture and Flow in Solids: Philosophical Transactions of the Royal Society of London, Series A, Containing Papers of a Mathematical or Physical Character, v. 221, p. 163-198.

Guo, F., N.R. Morgenstern, and J.D. Scott, 1993, Interpretation of Hydraulic Fracturing Pressure: A Comparison of Eight Methods Used to Identify Shut-in Pressure: Int. J. Rock Mech. Min. Sci. & Geomech., v. 30, p. 627-631.

Ihab, T., R. Naial, D.A. Moronkeji, J.A. Franquet, and S.S. Smith, 2014, Wireline Straddle Packer Microfrac Testing Enables Tectonic Lateral Strain Calibration in Carbonate Reservoirs: Paper IPTC-17301-MS, International Petroleum Technology Conference, Doha, Qatar, 20-22 January.

Jones, C., and J.P. Sargeant, 1993, Obtaining the Minimum Horizontal Stress from Microfracture Test Data: A New Approach Using a Derivative Algorithm: SPE Paper 18867, SPE Production and Facilities, February, 1993.

Lacy, L.L., 1997, Dynamic Rock Mechanics Testing for Optimized Fracture Designs: SPE Paper 38716, SPE Annual Technical Conference, San Antonio, 5-8 October.

Thiercelin M.J., R.A. Plumb, J. Desroches, P.W. Bixenman, J.K. Jonas, and W.A.R. Davie, 1993, A New Wireline Tool for In-Situ Stress Measurements: SPE Paper 25906, Rocky Mountain Region – Low permeability Reservoir symposium, Denver, 12-14 April. doi.org/10.2118/25906-PA

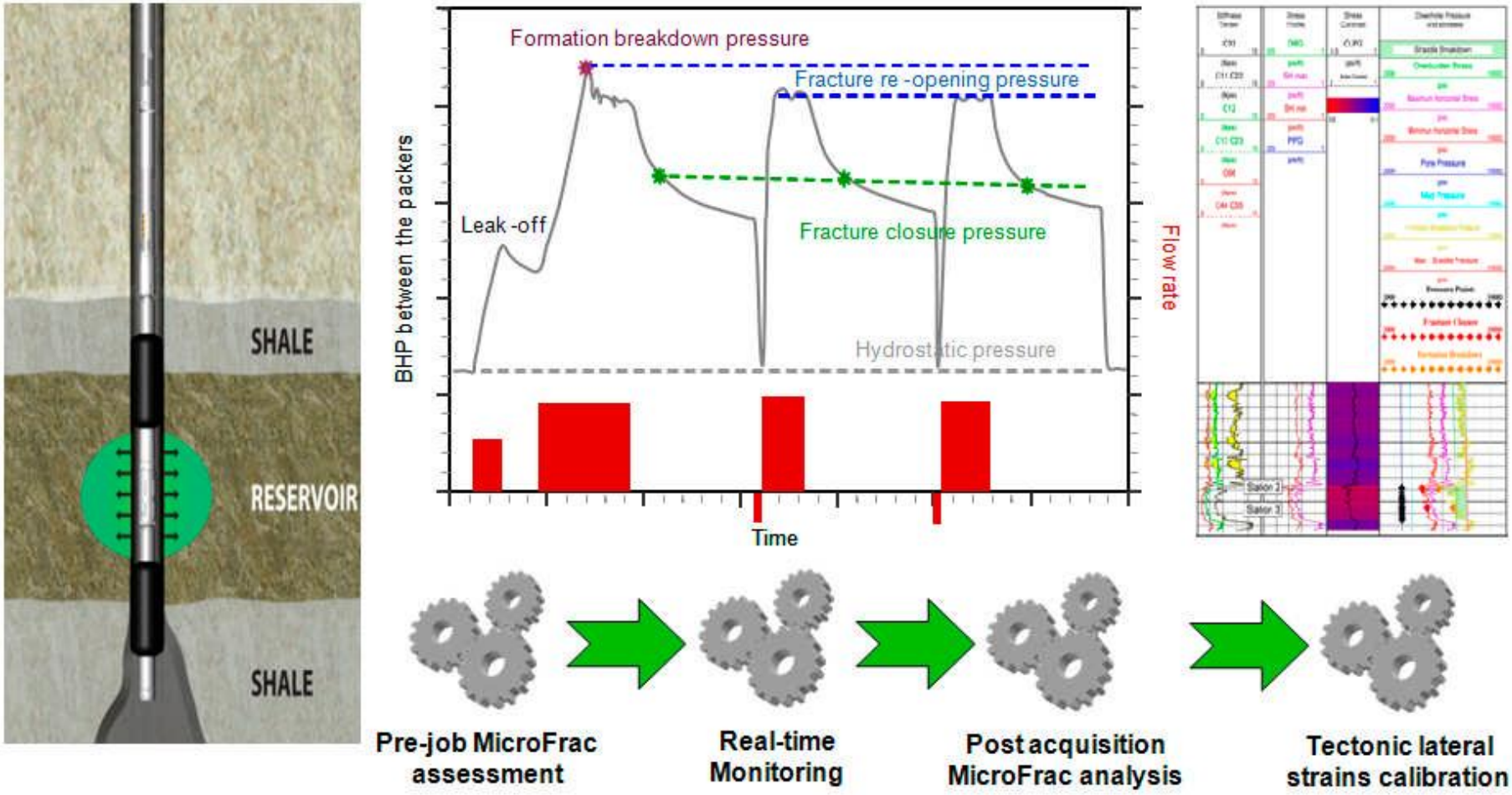

Figure 1. Straddle packer micro-fracture testing workflow.

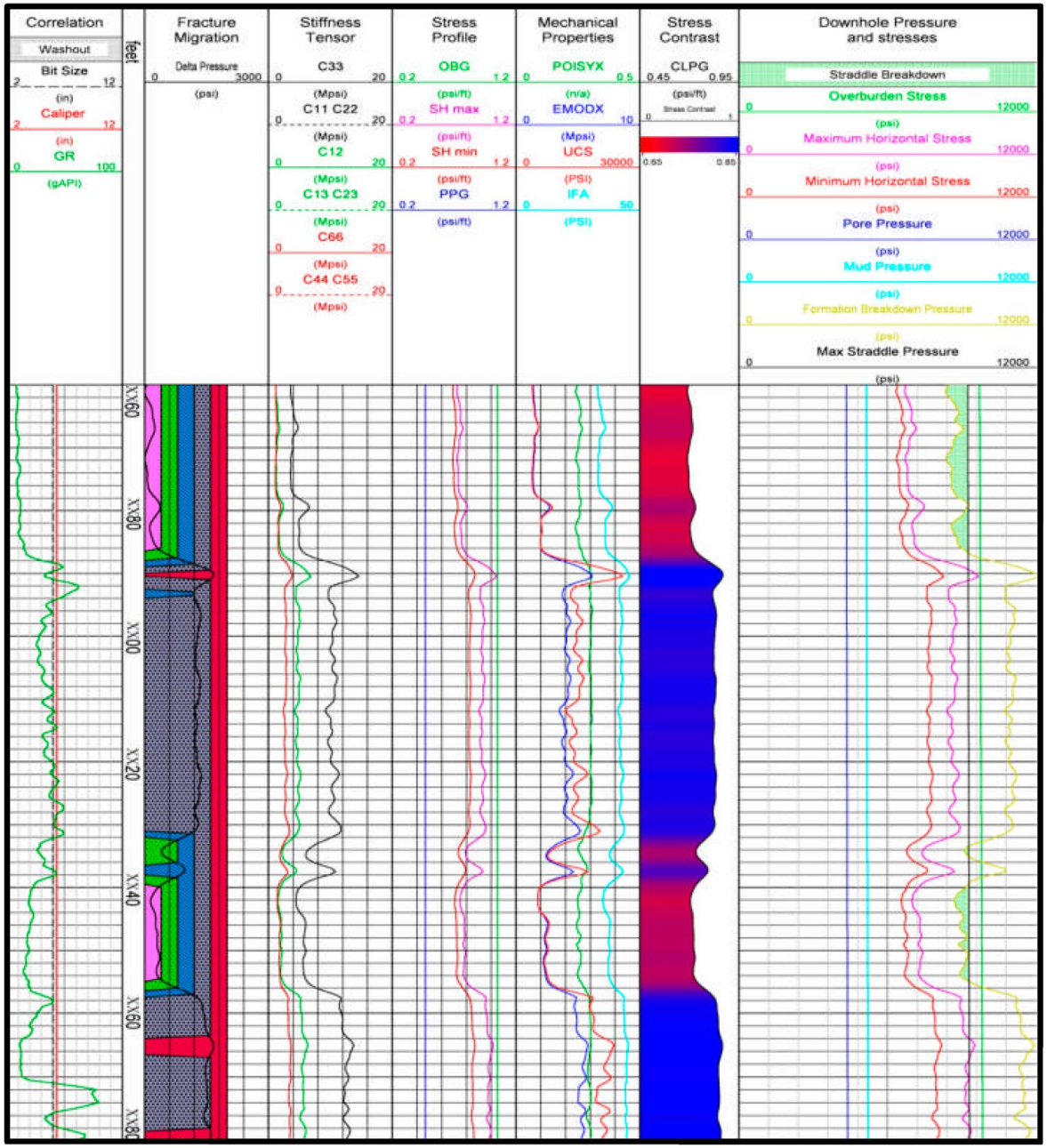

Figure 2. Pre-job micro-fracture assessment of an offset well.

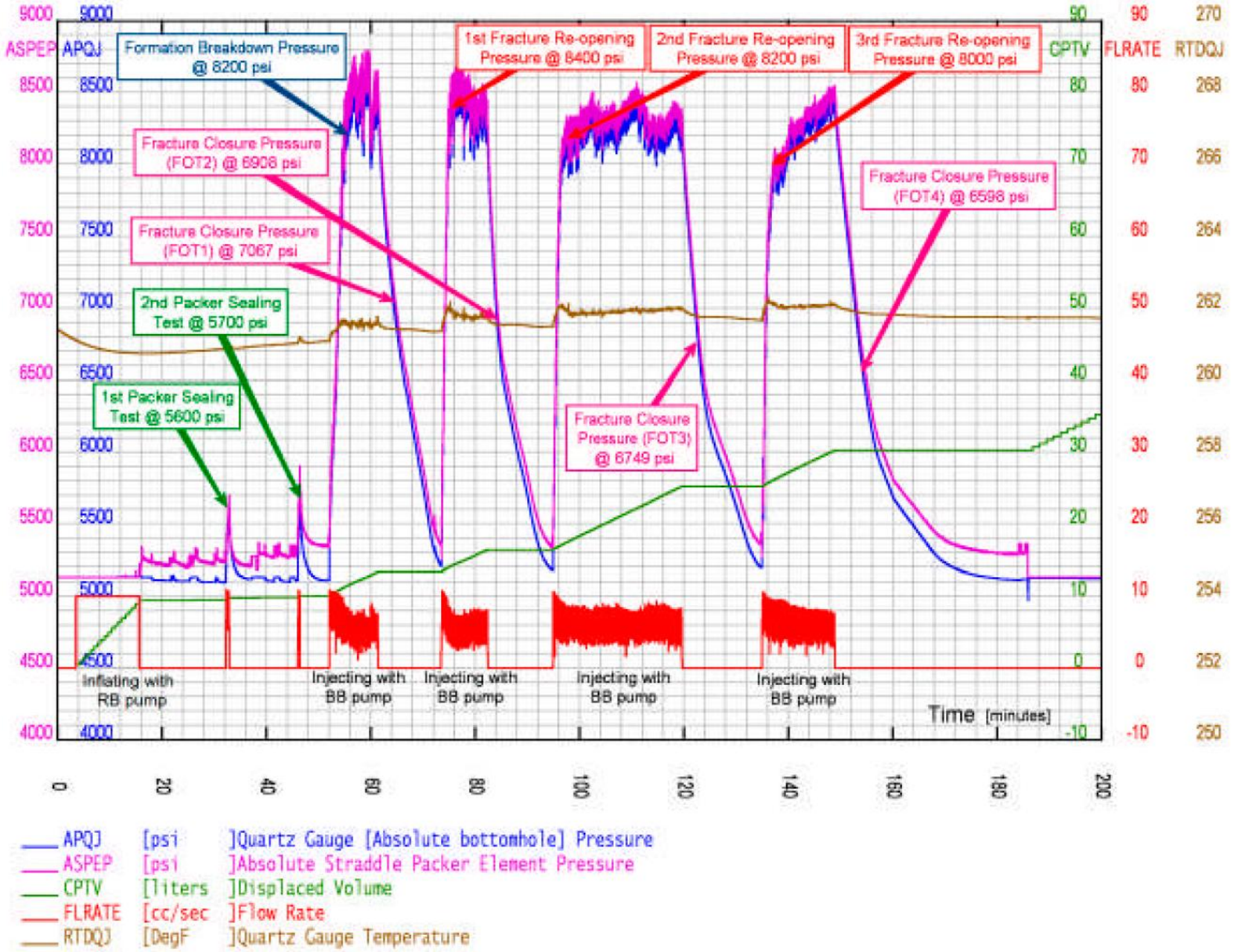

Figure 3. Micro-fracture test at Station 1.

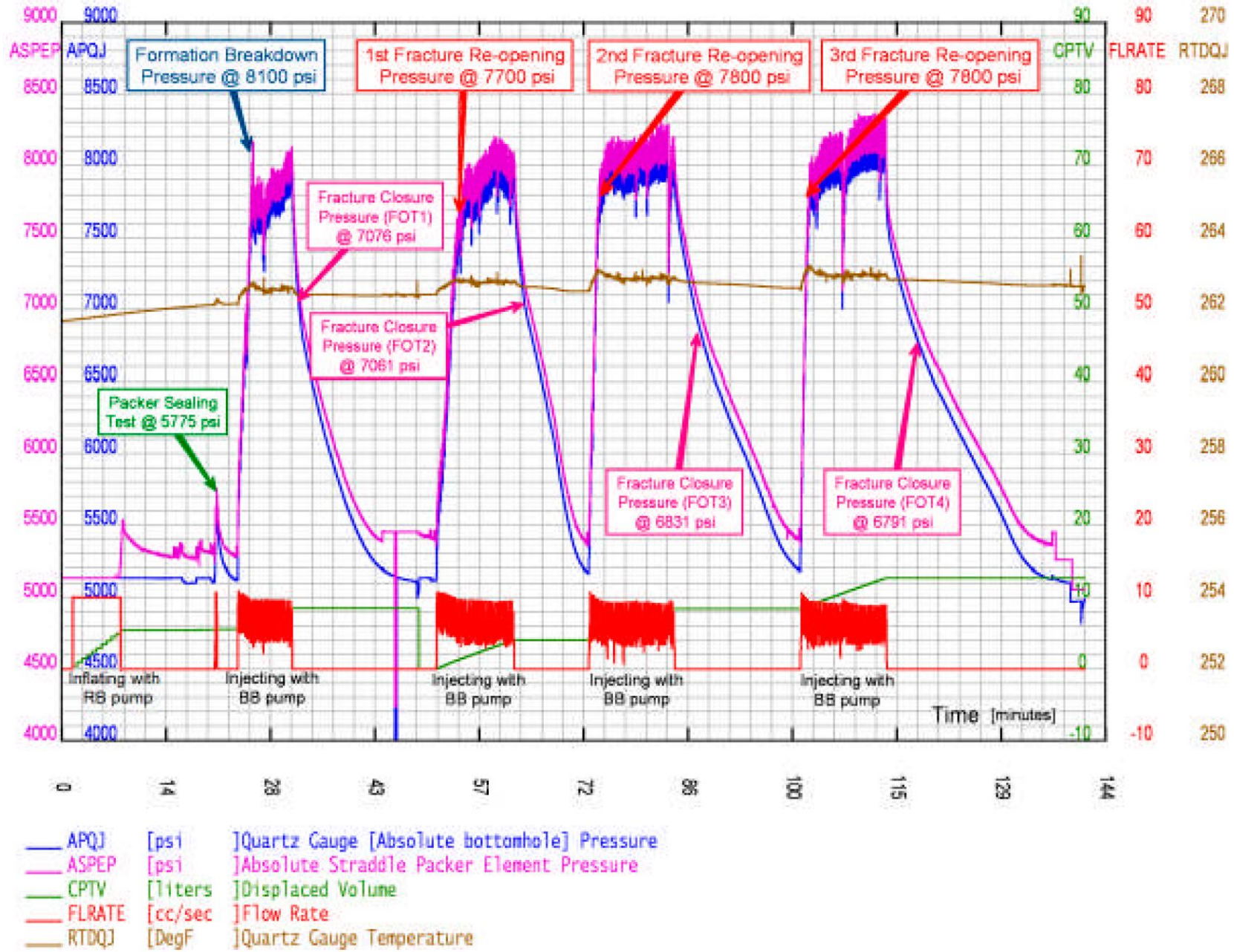

Figure 4. Micro-fracture test at Station 2.

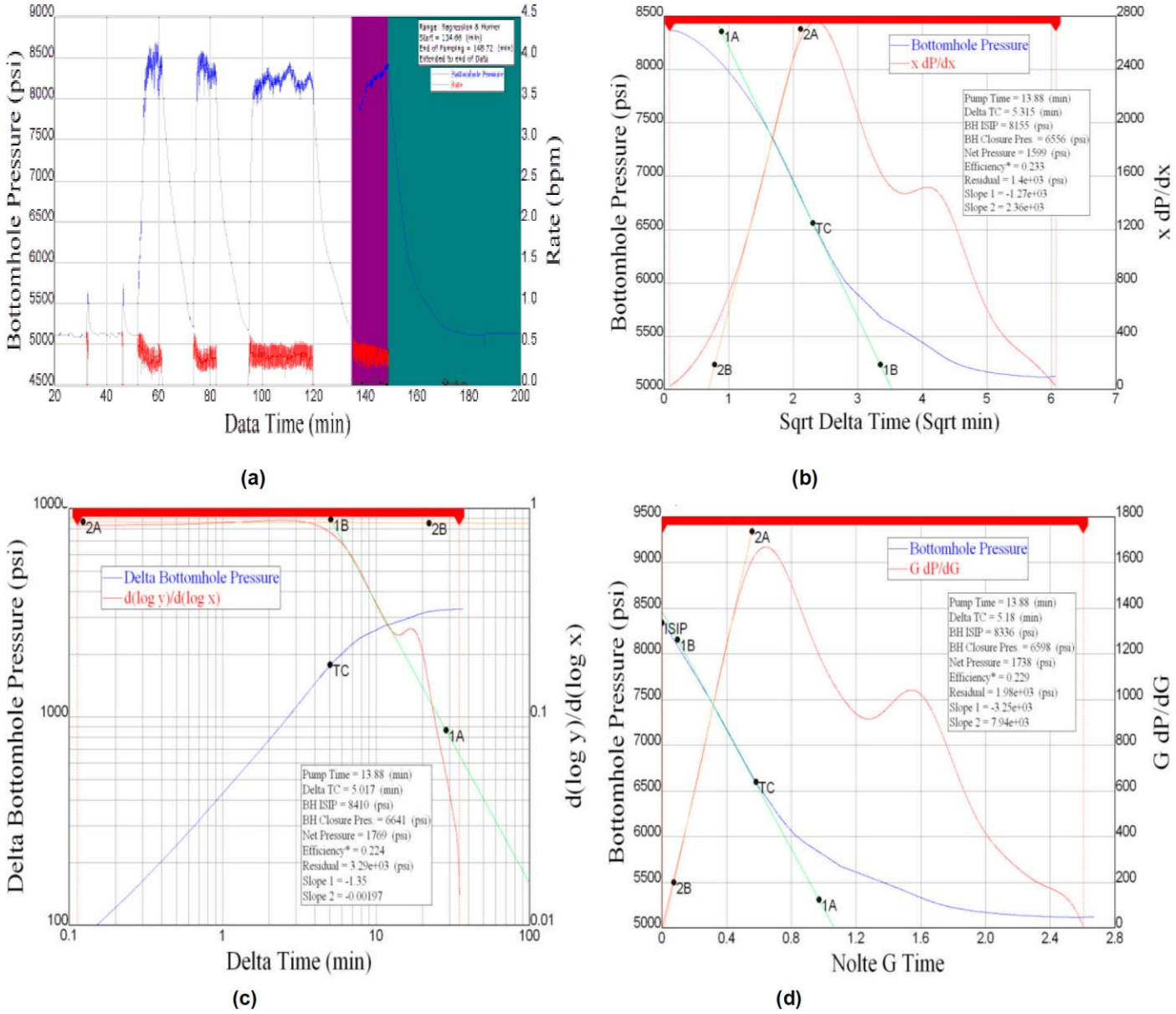

Figure 5. (a) Micro-fracture Station 1, Cycle 4. (b) Square-root of time fracture closure pressure analysis for fourth fall-off test (FOT4) at Station 1. (c) Log-log fracture closure pressure analysis (FOT4) at Station 1. (d) G-function fracture closure pressure analysis (FOT4) at Station 1.

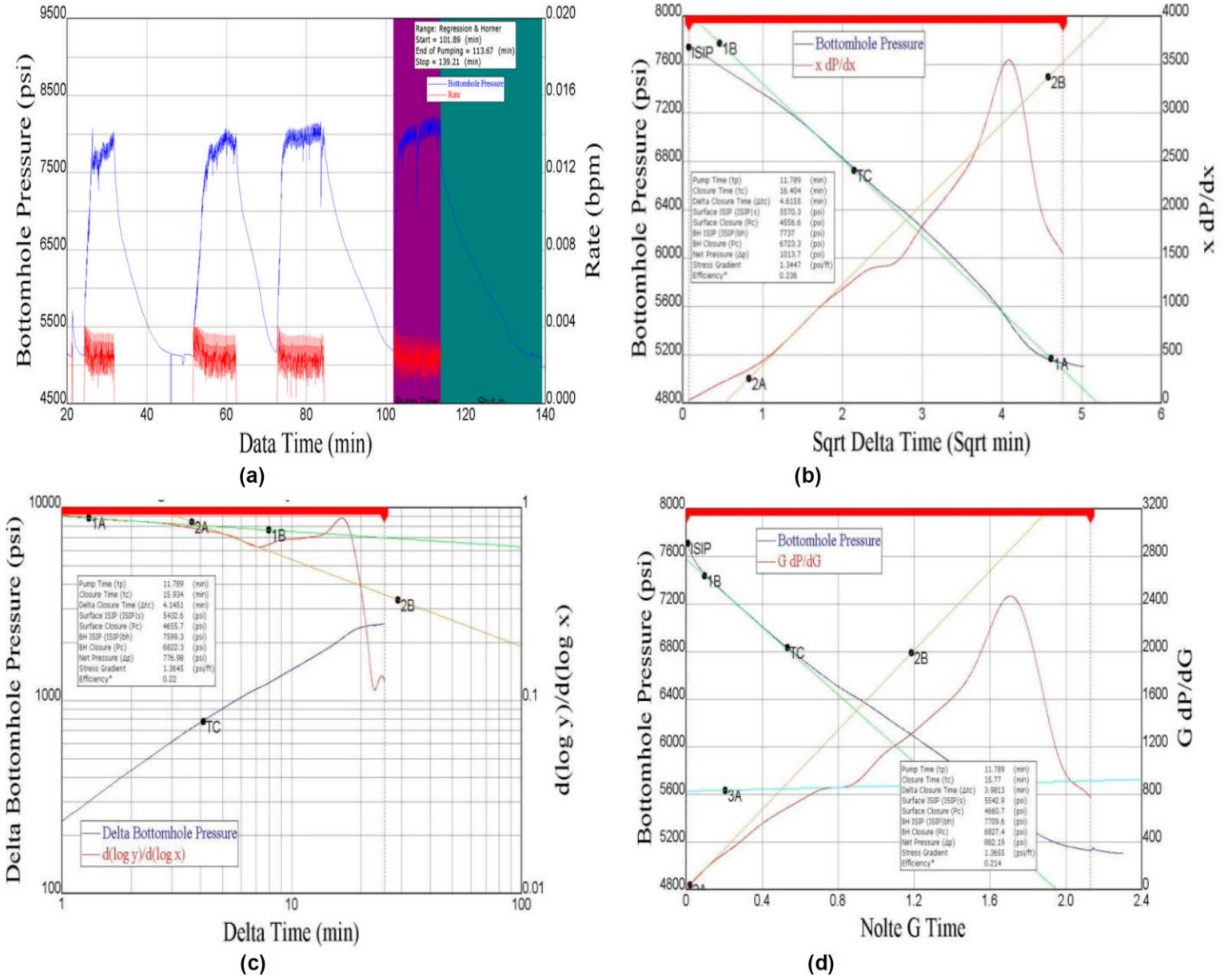

Figure 6. (a) Micro-fracture Station 2, Cycle 4. (b) Square-root of time fracture closure pressure analysis for fourth fall-off test (FOT4) at Station 2. (c) Log-log fracture closure pressure analysis (FOT4) at Station 2. (d) G-function fracture closure pressure analysis (FOT4) at Station 2.

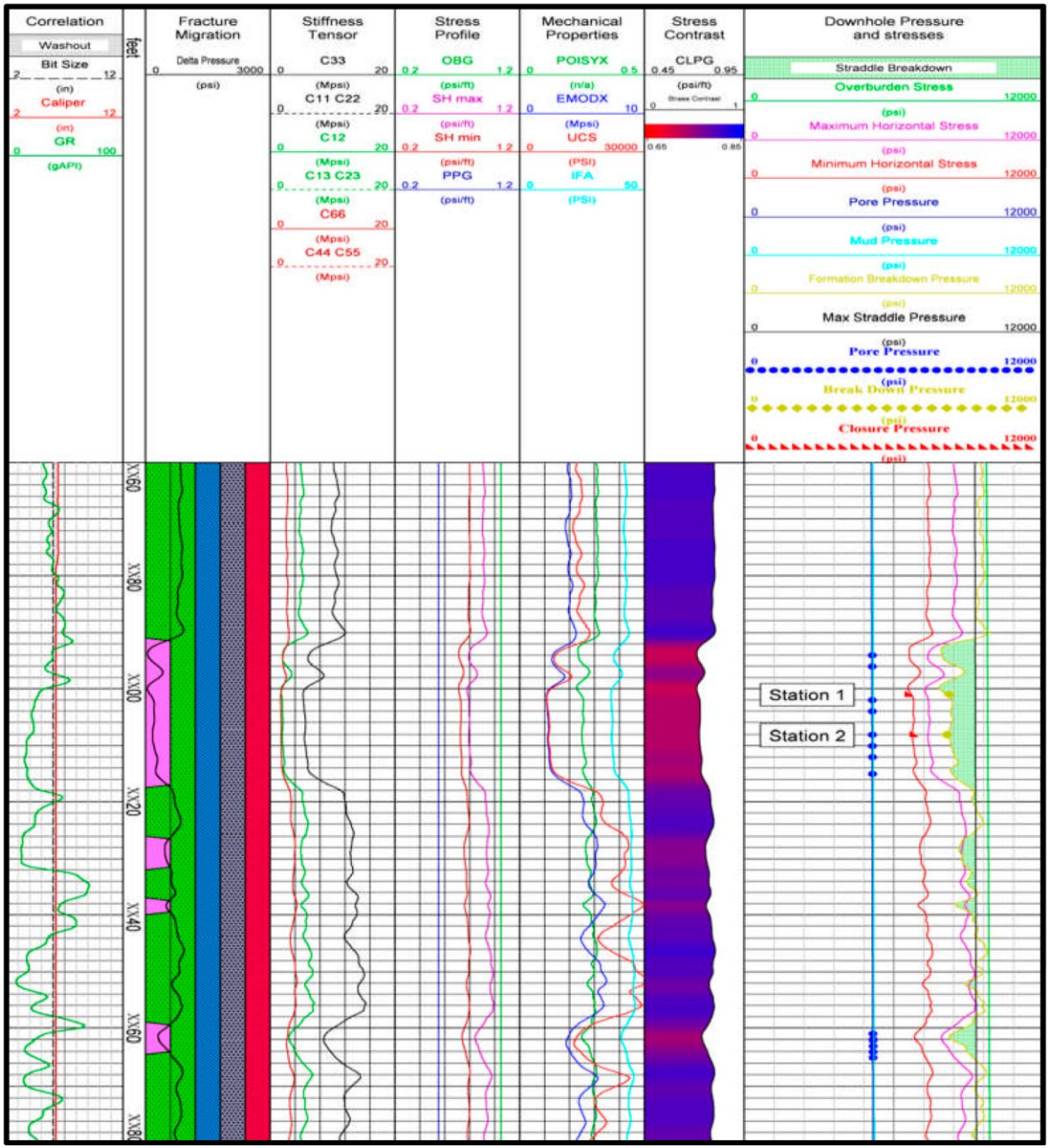

Figure 7. Post-job micro-fracture assessment.

Sequence of Operation	Injection Cycle	Formation Breakdown pressure [psia]	Reopening pressure [psia]	Propagation pressure [psia]	(SRT) Closure pressure [psia]	(Log-Log) Closure pressure [psia]	(G-Function) Closure pressure [psia]
Station 1	1	8200	-	8400	7021	7113	7067
	2	-	8400	8400	6870	6945	6909
	3	-	8200	8200	6680	6746	6822
	4	-	8000	8200	6556	6641	6598
Station 2	1	8100	-	7800	7051	7088	7090
	2	-	7700	7800	7041	7061	7080
	3	-	7800	8000	6767	6832	6893
	4	-	7800	8000	6723	6822	6827

Table 1. MicroFracture Pressure Decline Analysis Summary Results.